technical transactions

No. 2020/009

mechanics

sciendo

A vertical-axis rotor as the adjusting system of a horizontal axis wind turbine

Marcin Augustyn

augustyn@mech.pk.edu.pl | Orcid 0000-0002-8023-9198

Institute of Machine Design, Cracow University of Technology

Scientific Editor: Andrzej Sobczyk, Cracow University of Technology
Technical Editor: Aleksandra Urzędowska, Cracow University of Technology Press
Language Editor: Tim Churcher, Big Picture
Typesetting: Małgorzata Murat-Drożyńska, Cracow University of Technology Press

Received: October 25, 2019
Accepted: April 9, 2020

Data Availability Statement: All relevant data are within the paper and its Supporting Information files.

Competing interests: The authors have declared that no competing interests exist.

Citation: Augustyn, M. (2020). A vertical-axis rotor as the adjusting system of a horizontal axis wind turbine. *Technical Transactions, e2020009.* https://doi.org/10.37705/TechTrans/e2020009

Abstract

The proposed self-adjusting mechanism consists of a carousel rotor with a vertical axis consisting of two kinematically connected flat blades. The torque of this rotor can change the position of the directing unit and additionally the position of the main propeller in order to direct the wind stream or save the main rotor when the wind is too strong. The theory, principles of operation, and the properties of the self-adjusting system were illustrated by formulas and graphs. Based on research conducted in a boundary layer wind tunnel, the values of the aerodynamic coefficients of the flat blades were determined, and then the power and propeller torque of the rotor were found as a function of the angle of wind attack. A computational procedure provides kinematical and force relations as well as the resulting torque diagrams of the rotor. An example of the use and the design structure of a self-adjusting unit in the case of a horizontal axis wind turbine is presented.

Keywords: self-adjusting system, horizontal axis wind turbine, propelling torque, vertical axis wind turbine, wind rotor

1. Introduction

The popularity of wind turbines with a vertical axis of rotation VAWT (Vertical Axis Wind Turbine) is constantly growing. This geometry is increasingly used in large urban agglomerations and small households as an alternative source of energy, and in places where the only obtainable energy is from the wind. The ease of assembly of this type of turbine, producing the same power independently of the wind direction and the self-braking shape of the rotor that provides aerodynamic speed limitation, are compelling arguments for this type of construction (Hau, 2013). Therefore, there are new concepts for using VAWT, including visions of integrating such structures with urban spatial development plans and current architectural trends (Müller, Jentsch, Stoddart, 2009). There are numerous studies on wind flow simulations that influence the design of wind turbine structures to increase their efficiency (Bausas, Danao, 2015; Ferreira, Van Bussel, Van Kuik, Scarano, 2011; Howell, Qin, Edwards, Durrani, 2010). Other studies concern optimising the shape of the turbine rotor blade profiles (Ismail, Vijayaraghavan, 2015), their number (Li et al., 2015) changing the angular setting (Edwards, Danao, Howell, 2012; Hure et al., 2015) or guiding of the blades (Xisto, Pascoa, Trancossi, 2015).

However, a power plant having a main propeller with a horizontal axis, i.e. HAWT (Horizontal Axis Wind Turbine), has a higher efficiency in using wind energy than turbines with a vertical axis, as the main rotor is regulated by a rotor control system (Hau, 2013; Ahmed, 2011; Burton, Jenkins, Sharpe, Bossanyi, 2001) rather than by the propeller itself.

Among others, the following control methods can be distinguished:

- adjustment by setting the wind turbine in the direction of the wind (yaw control) (Dakin, Priyavadan, Hopkins, 2011; Islam, Ting, Fartaj, 2008).
- adjusting the rotor deviation (yaw regulation) – reducing the active surface of the rotor by deflecting the rotor axis away from the wind direction,
- blade pitch adjustment (active pitch regulation) (Dongran Song, et al., 2017; Kjellin, Eriksson, Bernhoff, 2013),
- adjustment by changing the load (load control) – changing the resistance to rotation.

This is the load on the generator. This approach is used in systems with a direct connection to the network, and in low-power wind turbine plants and it is very common (Rossander, Goude, Eriksson, 2017; Yang et al., 2016).

An interesting solution proposed by Wei (Wei, Pan, Liping, 2015) is a wind turbine rotor with three blades with folding outer blade sections to control the power output. When the outer blade section is folded, a decrease of both the blade energy conversion efficiency and wind energy extracted from the airflow that passes through the rotor leads to a reduction in the power output.

The preferred solution is the use of a self-adjusting system which uses wind energy to operate. This paper concerns such a solution (Eriksson, Bernhoff, Leijon, 2008; Pope, Dincer, Naterer, 2010).

Taking the above into account, a concept was created and designed to combine the advantages of both types of wind turbines. Therefore, a new method of rotational speed control and wind turbine guidance for HAWT is proposed, using a second rotor with a vertical axis for this purpose. The wind turbine with a vertical axis of rotation is presented as a completely new aspect. The aim of this work is to use experimental data and theoretical calculations as well as to analyse the design and operation of the proposed solution in order evaluate it compared to HAWT turbine adjustment systems.

https://doi.org/ 10.37705/TechTrans/e2020009

2. The theory and principles of operation of the adjusting system

For the proposed solution, the theoretical calculations of the propelling torque M per 1m² of the turbine blade area [Nm/m²] of the rotor adjusting system as a function of the angle of wind attack β was made. A structure and a principle of operation was described in the next part of the article.

The rotor adjusting system consists of a turbine with two flat blades, positioned so that the axes of the cross-sections of the blades are perpendicular to each other. It should be noted that the blades are moving in planetary motion (gear ratio $i = 1/2$) and the adjusting system changes the orientation of the blades with respect to the system's neutral position (Fig. 1a). When there is sufficient wind, the blades adjust to the active position (Fig. 1b), which deflects the turbine when the main rotor speed (HAWT) exceeds the limit value (Ryś, Augustyn, 2015). In this case, the blades are changing positions relative to each other via rotation around their own axis by an angle of 45°, corresponding to the main rotor speed (HAWT) exceeding the limit value (Ryś, Augustyn, 2015). They will remain in this position until the rotation of the main rotor falls to an acceptable value. Theoretical calculations for the active position are unnecessary, because in both cases the operation of the self-adjusting system mechanism is the same and the difference during the start time is due to the orientation of the blades to the wind direction - in the active position, the propelling torque is the largest.

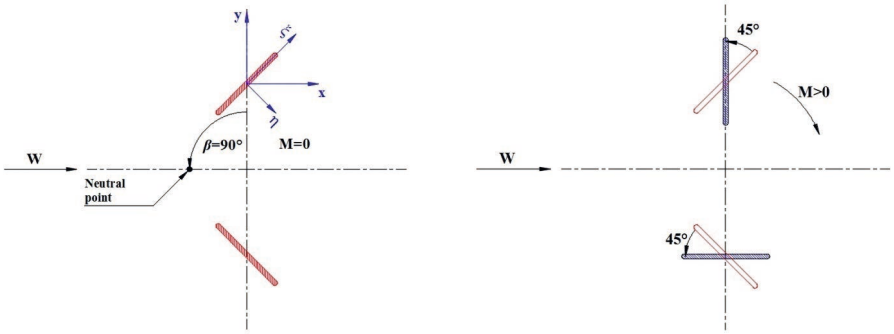

Fig. 1. Position of the self-adjusting turbine blades: (a) neutral and (b) active

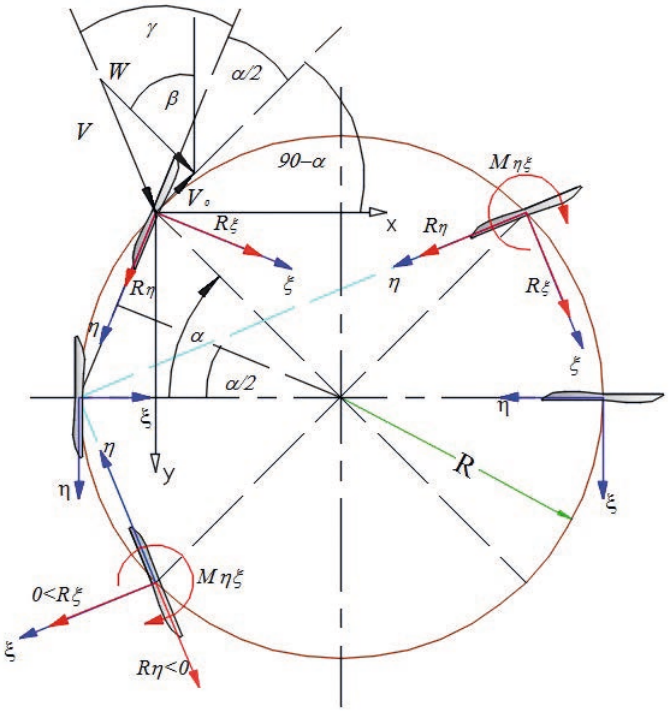

Fig. 2. Scheme of the forces acting on the single rotor blade for the selected positions relative to the rotor axis (VAWT); R_ξ, R_η and $M_{\eta\xi}$ – the forces and the torque acting on the blade in the moving coordinate system ξ and η; α – the angle of the rotor rotation, and the position of the blade relative to the rotor α=0–2π [rad] ($\alpha = \alpha_s$ in numerical calculations [°]); R – the radius from the rotor axis to the blade axis [m], γ – the angle of the wind attack on the turbine blade γ= α/2 [°]; β – the angle of the wind stream operation relative to the rotor [°]

According to Fig. 2, the procedure for calculating the propeller torque and computing power of the rotor with a self-adjusting system as a function of the angle of wind attack were prepared.

The resultant torque for the self-adjusting turbine is the sum of the torque generated by the first and second rotor blade:

$$M(\alpha_s) = M_1(\alpha_s) + M_2(\alpha_s) \tag{1}$$

The propeller torques from both blades are given by the following formulas:

$$M_1(\alpha_s) = \left(M_{1\eta\xi}(\alpha_s) + M_{1\xi}(\alpha_s)\right) - M_{1\eta}(\alpha_s) \tag{2}$$

$$M_2(\alpha_s) = \left(M_{2\eta\xi}(\alpha_s) + M_{2\xi}(\alpha_s)\right) - M_{2\eta}(\alpha_s) \tag{3}$$

where, the torques $M_{\eta\xi}$, M_{ξ}, M_{η} from the first blade in the moving coordinates ξ and η are described by the equations:

$$M_{1\eta\xi}(\alpha_s) = 0.5\left(\frac{V_\eta(\alpha_s)}{W}\right)^2 \cdot k_{\eta\xi} \tag{4}$$

$$M_{1\zeta}(\alpha_s) = \left(\frac{V_\zeta(\alpha_s)}{W}\right)^2 \cdot k_\zeta \cdot \sin\left(\frac{\alpha(\alpha_s)}{2}\right) \cdot sign\left(V_\zeta(\alpha_s)\right) \tag{5}$$

$$M_{1\eta}(\alpha_s) = s_{\eta\xi}\left(\frac{V_\eta(\alpha_s)}{W}\right)^2 \cdot k_\eta \cdot \cos\left(\frac{\alpha(\alpha_s)}{2}\right) \cdot sign\left(\cos\left(\frac{\alpha(\alpha_s)}{2}\right)\right) \tag{6}$$

and the torques generated from the second rotor blade:

$$M_{2\eta\xi}(\alpha_s) = 0.5\left(\frac{V_\eta(\alpha_s + 180)}{W}\right)^2 \cdot k_{\eta\xi} \tag{7}$$

$$M_{2\xi}(\alpha_s) = \left(\frac{V_\eta(\alpha_s + 180)}{W}\right)^2 \cdot k_\xi \cdot \sin\left(\frac{\alpha(\alpha_s + 180)}{2}\right) \cdot sign\left(V_\xi(\alpha_s + 180)\right) \tag{8}$$

$$M_{2\eta}(\alpha_s) = s_{\eta\xi}\left(\frac{V_\eta(\alpha_s + 180)}{W}\right)^2 \cdot k_\eta \cdot \cos\left(\frac{\alpha(\alpha_s + 180)}{2}\right) \cdot sign\left(\cos\left(\frac{\alpha(\alpha_s + 180)}{2}\right)\right) \tag{9}$$

The remaining values in the equations are the relative velocity components V_η and V_ξ [m/s] for the moving coordinates system associated with turbine blades ξ and η:

$$V_\xi = W\sin\left(\frac{\alpha_s}{2} + \beta\right) - V_0 \sin\frac{\alpha_s}{2} \tag{10}$$

$$V_\eta = W\cos\left(\frac{\alpha_s}{2} + \beta\right) + V_0 \cos\frac{\alpha_s}{2} \tag{11}$$

where, the wind speed is W [m/s], the rotor speed is V_o [m/s], the angle of the rotor rotation is α_s, the mean value of the aerodynamic coefficients are k_η, k_ξ, $k_{\eta\xi}$ related to the moving coordinate system ξ–η and current rotor blade contour (ratio of frontal surface to lateral surface of the blade) $s_{\eta\xi}$.

https://doi.org/ 10.37705/TechTrans/e2020009

3. Aerodynamic test

Aerodynamic tests of the blade system were carried out to determine the mean value of the aerodynamic coefficients, related to the wind speed components k_η, k_ξ, $k_{\eta\xi}$ relative to the blade. The experimental tests were conducted in the boundary layer wind tunnel of the Wind Engineering Laboratory at the Cracow University of Technology. For this purpose, an appropriate rigid blade with a self--adjusting rotor was made.

The dimensions of the measuring space: width 2.2 m; height – ranging from 1.4 m at the beginning to 1.6 m at the end of the measurement space, and a length of 10 m.

Formation of the wind speed and atmospheric turbulence profile takes place in the first part of the measurement space, with a length of over 6 m, using a suitable turbulence grid, barriers, spires and blocks with appropriate geometry and spacing as well as mechanically adjustable heights.

Due to the dimensions of the tunnel's measuring space, the dimensions of the blades had the following values: a = 0.25 m (width of the blade), b = 0.06 m (length of the blade) and h = 0.65 m (height of the rotor blade – rectangular shape). For the assumed dimensions of the tested blade, the geometric scale k_D is 1/1; therefore, a section to determine other similar criteria is not needed.

The basic characteristics of measurement parameters (Flaga, Kłaput, Augustyn, 2016) are shown in Table 1.

Table 1. Characteristics of measurement parameters

Terrain roughness category	Flat urban terrain
Geometric scale k_D	1:1
Mean values of wind speed W_{ref}	17.4 m/s
Mean value of dynamic pressure q_{ref}	187.2 N/m^2
Mean turbulence intensity of wind velocity I_W[%] on the top of the blade	14.7%
Number of considered wind directions	18 (0°-180°)
Measurement of reference pressure	On the height level of the tested blade

Turbulence intensities $I_W(h)$ were calculated according to the formula:

$$I_W(h) = \frac{\sigma(h)}{W(h)} \tag{12}$$

where: $W(h)$ – mean values, $\sigma(h)$ – standard deviations and h – height of the tested blade.

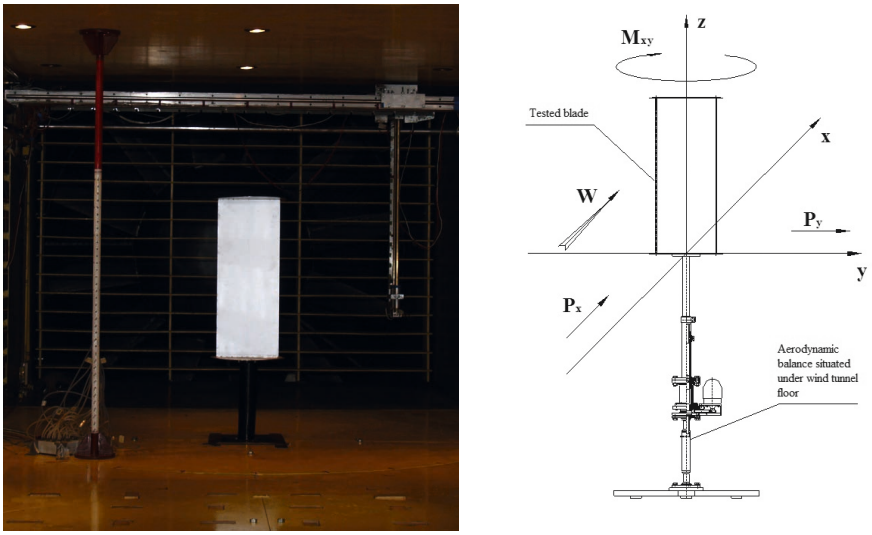

Fig. 3. Tested blade in the tunnel test (a) and scheme of aerodynamic balance and components of wind action on an object (b)

The wind speed measurement was carried out using a set of pressure scanners. The pressure sensors are placed in a vertical plane as shown in Fig. 3a.

For the tested blade, the aerodynamic moment M_{xy} and aerodynamic forces P_x and P_y have been measured using the three-component aerodynamic balance based on the electric resistance strain gauges (Ryś, Augustyn, 2013). The orientation of the fixed coordinate system x, y, z is as follows: x – along wind direction; y – across wind direction; z – vertical direction (Fig. 3b).

For calculations of the forces R_η, R_ξ and the moment $M_{\eta\xi}$ in the system η, ξ; $\gamma = \alpha/2$ with gamma fixed for peripheral speed $V_o = 0$ and $\beta = 0$ one finds:

$$R_\eta = P_x \cos\left(\frac{\alpha}{2}\right) - P_y \sin\left(\frac{\alpha}{2}\right) \tag{13}$$

$$R_\xi = P_x \sin\left(\frac{\alpha}{2}\right) - P_y \cos\left(\frac{\alpha}{2}\right) \tag{14}$$

$$M_{\eta\xi} = M_{xy} \tag{15}$$

The values obtained from the measurements and the calculated values of forces R_η, R_ξ are summarised in Table 2.

Table 2. The values of aerodynamic forces and aerodynamic moment, for fixed conditions x, y, z and values of gamma; The resulting aerodynamic forces and aerodynamic moment in moving coordinate system η, ξ

xy				$\eta\xi$	
γ [°]	P_x	P_y	$M_{\eta\xi} = M_{xy}$	R_η	R_ξ
0	2.79	-0.81	-0.09	2.79	-0.81
10	6.35	10.56	0.17	4.42	11.50
20	8.63	10.82	0.19	4.40	13.12
30	11.36	10.94	0.13	4.37	15.15
40	14.52	11.09	0.13	4.00	17.83
50	17.73	10.73	0.03	3.17	20.48
60	20.95	9.87	0, 00	1.93	23.08
70	23.47	7.72	-0.03	0.77	24.70
80	24.83	5.03	-0.07	-0.64	25.33
90	25.16	1.80	-0.11	-1.80	25.16
100	24.72	-1.63	-0.15	-2.68	24.63
110	23.06	-4.81	-0.18	-3.37	23.32
120	20.43	-7.77	-0.19	-3.49	21.58
130	16.73	-9.33	-0.19	-3.60	18.82
140	11.78	-11.41	-0.19	-1.69	16.32
150	8.64	-12.02	-0.18	-1.47	14.73
160	5.90	-13.66	-0.16	-0.87	14.85
170	2.74	-7.61	-0.22	-1.37	7.97
180	2.71	-0.81	-0.03	-2.71	0.81

The obtained values of aerodynamic forces and moment in the moving coordinate system ξ and η (R_η, R_ξ, $M_{\eta\xi}$) was used to determine the coefficients k_η, k_ξ, $k_{\eta\xi}$. The coefficients were described by the following equations and are shown as a function of the attack angle in Fig. 4–6:

$$k_\eta = \frac{R_\eta}{q_{ref} \cdot s_{\eta\xi}} \tag{16}$$

https://doi.org/ 10.37705/TechTrans/e2020009

$$k_{\xi} = \frac{R_{\xi}}{q_{ref} \cdot s_{\eta\xi}} \tag{17}$$

$$k_{\eta\xi} = \frac{M_{\eta\xi}}{q_{ref} \cdot s_{\eta\xi} \cdot a} \tag{18}$$

$$q_{ref} = \frac{1}{2}\rho W_{ref}^2 \tag{19}$$

where:
ρ is the density of the air [kg/m^3];

The surface area $s_{\eta\xi}$ [m^2] (Fig. 7) of the cuboid's self-adjusting turbine blade for the moving rotor was described in the following way:

$$s_{\eta\xi} = \left(a \cdot \sin\left(\frac{\alpha_s}{2}\right) + b \cdot \cos\left(\frac{\alpha_s}{2}\right) \cdot sign\left(\cos\left(\frac{\alpha_s}{2}\right)\right)\right) \cdot h \tag{20}$$

The current contour area sn_{ξ} of the tested blade was calculated from the product of the blade height to the perpendicular projection of its contour, depending on the setting of the blade in the x, y system (Fig. 2) during operation of the rotor together with the coordinate system ξ and η. The rotor blades rotate with respect to their own axis in the opposite direction and at twice the speed of rotation relative to the rotor. This is possible due to the use of a planetary gear in this constructional solution.

The values of the surface area $s_{\eta\xi}(\alpha_s)$ in the moving coordinate system ξ and η were presented in a graphical manner (Fig. 7).

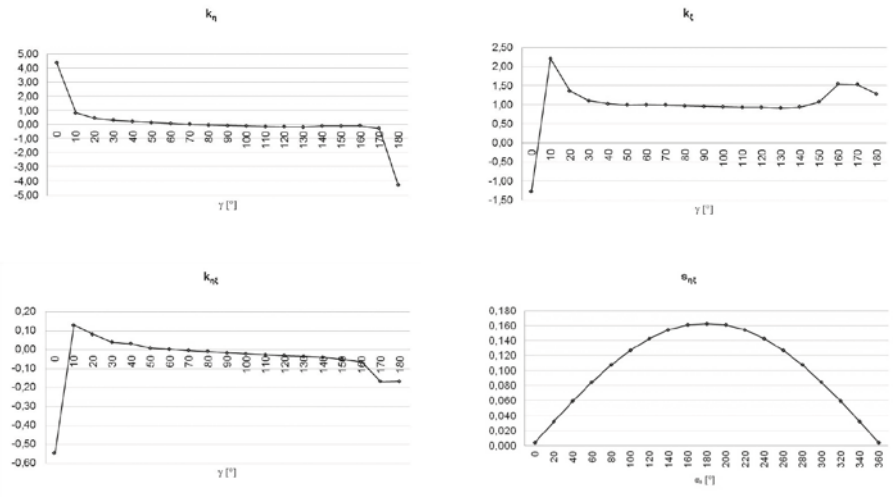

Fig. 4. Aerodynamic coefficient value k_{η} as a function of the angle of wind attack on the turbine blade γ
Fig. 5. Aerodynamic coefficient value k_{ξ} as a function of the angle of wind attack on the turbine blade γ

Fig. 6. Aerodynamic coefficient value $k_{\eta\xi}$ as a function of the angle of wind attack on the turbine blade γ

Fig. 7. The values of the surface area $s_{\eta\xi}$ a function of angle of the rotor rotation α_s

4. Principles of operation of the self-adjusting system and interpolation of the propelling torque

In the calculation of the torques, the mean values of the aerodynamic coefficients and the mean value of the surface area were adopted: k_{η}=0.8; k_{ξ}=1; $k_{\eta\xi}$=0; $s_{\eta\xi}$=0.1.

The propelling torque is:

$$M = I \cdot \rho \cdot R \cdot W^2 \tag{21}$$

where R is the radius of the turbine and I is the mean torque of the self-adjusting turbine with two blades [Nm]:

$$I = \frac{\left(\int_0^{360} M(\alpha_s)d\alpha_s\right)}{360} \tag{22}$$

Power N [W] per one square metre of the self-adjusting turbine blade (ω – angular velocity of the rotor) is given by:

$$N = M \cdot \frac{V_0}{R} = M \cdot \omega \tag{23}$$

The characters in the formula (23) indicate the rotor speed: (+) refers to ω>0, (–) refers to ω<0 (Fig. 8).

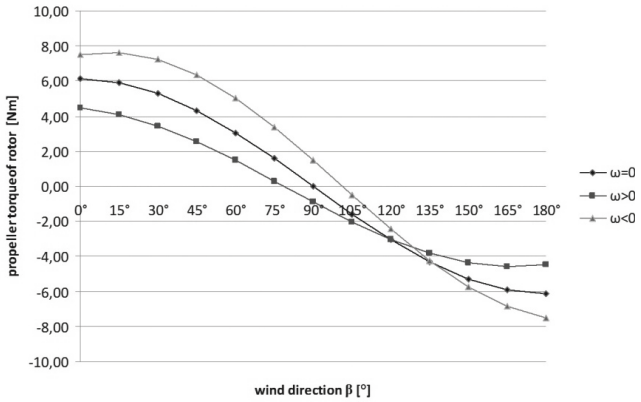

Fig. 8. The values of the propeller torque $M(\beta)$ per 1m² of the blade for the two flat symmetrical blades of the rotor adjusting system as a function of the angle of wind attack β: W=5 [m/s]; R=0.3 [m]

Two cases were considered in the calculations. The first case was for the rotor speed of the self-adjusting turbine equal to zero V_o=0 [m/s] with three different angles of wind attack β, while the second case was for the speed of the self-adjusting rotor which shall be different from zero V_o=1 [m/s] and also the four different wind directions. In both cases, the wind speed is W=5 [m/s].

The examples of the values of torque and power from the computing procedure in tabular form are shown below in Table 3.

Table 3. The values of torque M and power N of the self-adjusting turbine onto the direction of the wind, depending on the wind direction β for rotor turbine speed V_o=1 (ω>0), V_o=0 (ω=0) and V_o= –1 (ω<0)

	β	0°	78.5°	90°	101.5°	180°
V_o=1 (ω>0)	M [Nm]	3.911392	-0.003785	-1.246515	-2.582774	-8.800632
	N [W]	13.037973	-0.012618	-4.155051	-8.609248	-29.335439
V_o=0 (ω=0)	M [Nm]	6.11155	-	0	-	-6.11155
	N [W]	0	-	0	-	0
V_o= –1 (ω<0)	M [Nm]	8.800632	2.582774	1.246515	-0.003785	-3.911392
	N [W]	-29.335439	-8.609248	-4.155051	-0.012618	13.037973

The propeller torque of the self-adjusting turbine $M(\beta)$, for the constant value of the radius of the rotor equal to R=0, 3 [m] as a function of the angle of wind attack β (Fig. 8) is given by the following empirical form:

$$M(\beta) = M_0(W) \cdot \left[1 - \frac{5}{4} \cdot \frac{V_0}{W}\right] \cdot \cos \cdot \left[\beta + arctg\frac{V_0}{W}\right] \tag{24}$$

$$M_0(W) = 0.2445 \cdot W^2 \tag{25}$$

The propeller torque of the self-adjusting turbine $_M(_\beta)$ for any value of the rotor radius $_R$ at the function of the angle of the wind attack on the rotor $_\beta$:

https://doi.org/ 10.37705/TechTrans/e2020009

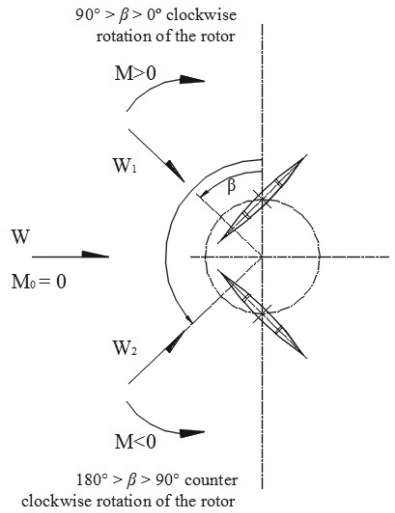

Fig. 9. Scheme illustrating the direction of rotation of the self-adjusting rotor during the change of the wind direction from W_1 to W_2 – neutral position

$$M(\beta) = m_0 W^2 \cdot \left[1 - \frac{5}{4} \cdot \frac{V_0}{W}\right] \cdot \cos \cdot \left[\beta \pm actg \frac{V_0}{W}\right] \tag{26}$$

$$m_0 = 0.2445 \frac{R}{0.3} \tag{27}$$

In the case, when 90° > β > 0° the torque on the directional rotor is positive (clockwise rotation of the rotor), when 180° > β > 90°, the torque is negative (counter clockwise rotation of the rotor) as was shown in Fig. 9.

With this arrangement, any change of the wind direction causes the resultant force to tilt and the emergence of the torque on the axis of the turbine. The torque of the self-adjusting gear, transferred to the bearing structure, provides an adjusting displacement in the direction of reducing the angle between the axis of the main rotor jib of the turbine nacelle, to which the rotor of the self-adjusting turbine is attached, as well as the wind direction.

The obtained results allow us to illustrate the principle operation of the self-adjusting rotor, as was shown in Fig. 10 and Fig. 11.

A change from a blade position angle of 45° in the neutral position (Fig. 1a) to the active position (Fig. 1b) results in the self-adjusting system exhibiting a positive or negative value of the propeller torque (Fig. 12), depending on the setting of the self-adjusting system mechanism (a position change of the blades is forced by an electromagnetic actuator or stepper motor) (Ryś, Augustyn, 2015), thanks to which the system can adjust the main rotor of the turbine to the new position by changing the angle of the main rotor axis to the wind direction to unfavorable.

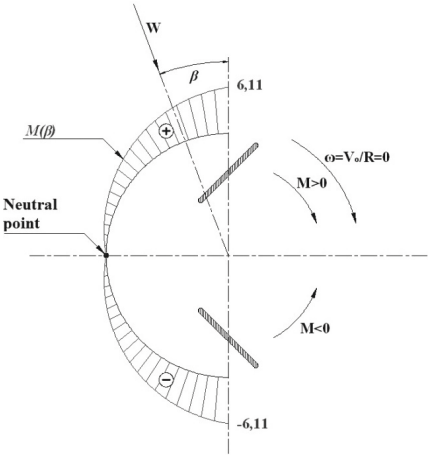

Fig. 10. Graph of the propeller torque for two flat symmetrical blades of the self-adjusting system as a function of wind direction $M(\beta)$: W=5 [m/s]; R=0.3 [m]; V_o=0 [m/s]; V_o/W=0

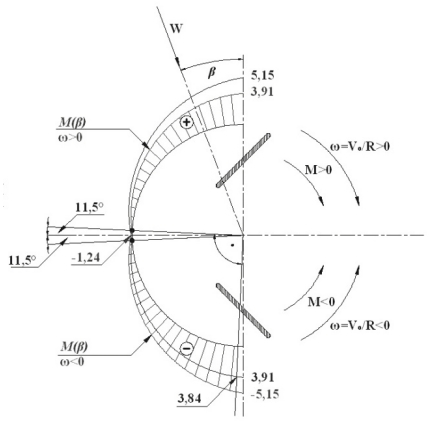

Fig. 11. Graph of the propeller torque for two flat symmetrical blades of the self-adjusting system as a function of wind direction $M(\beta)$: W=5 [m/s]; R=0, 3 [m]; V_o=1 [m/s]; V_o/W=0.2

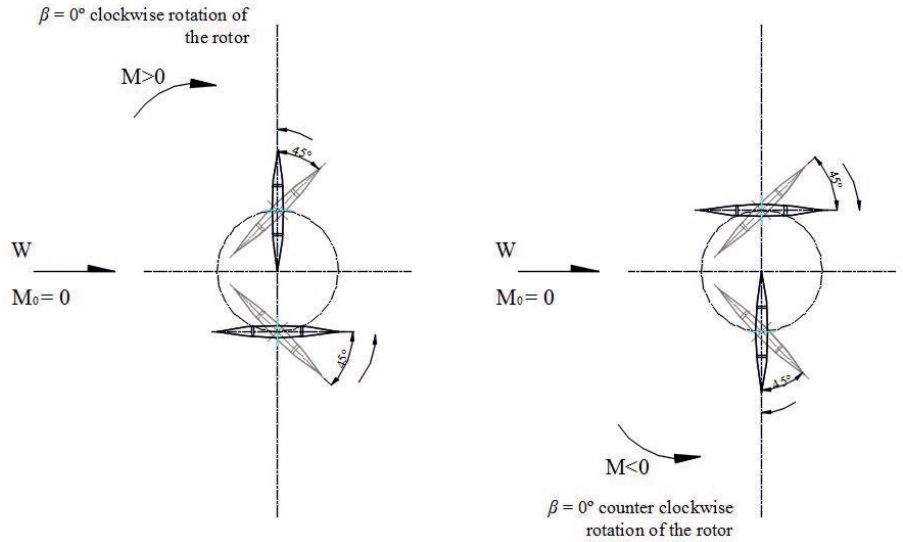

Fig. 12. Scheme illustrating the direction of rotation of the self-adjusting rotor depending on the setting of the self-adjusting system mechanism – active position

5. Example of the use of the self-adjusting turbine

The properties described above allow the protection of the main rotor of a HAWT against excessive speed in strong winds. The design solution of the self-adjusting system (Ryś, Augustyn, 2015) enabling the technical implementation of the concept discussed above is shown in Fig. 13.

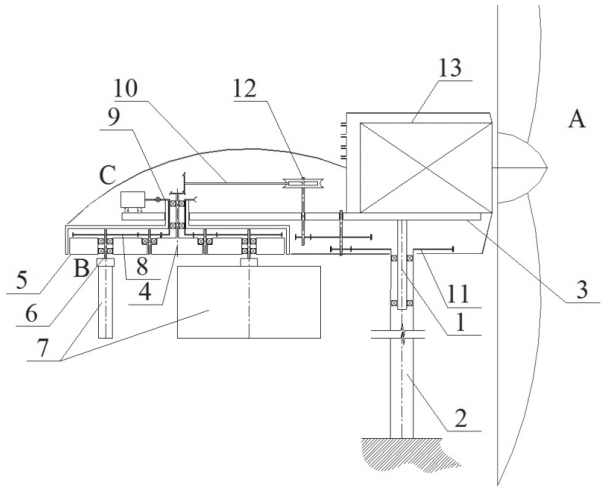

Fig. 13. Kinematic scheme of the horizontal axis turbine with the self-adjusting system, where: A – main rotor of the horizontal axis wind turbine, B – rotor of the self-adjusting turbine with the planetary motion of the two-blades adjusting the horizontal axis wind turbine to the wind direction, C – electromagnetic actuator or stepper motor of the self-adjusting system, which forces a change to the position of the blades, 1 – shaft of the nacelle mounted with bearings on the supporting structure, 2 – supporting structure of the horizontal axis wind turbine (flagpole), 3 – jib of the self--adjusting system, 4 – axis of the adjusting rotor, 5 – supporting beam of the adjusting rotor, 6 – axis of the lobe of the adjusting rotor, 7 – lobe (blade) of the adjusting rotor, 8 – transmission gears with a ratio of 1:2, 9 – self-locking worm gear, 10 – bevel gear, 11 – gear wheel mounted on the supporting structure, 12 – self-locking worm gear, 13 – generator of the main rotor

In the presented solution, the carousel rotor is used as the directional rotor B, mounted on a jib 3. The rotor is equipped with an even number of airfoils 7, whose axles are connected by the transmission gears 8 to the worm gear 9. The system is connected to the stepper motor C, whose task is to protect the main rotor A against strong wind. When the speed of the main rotor rises to 380, and the voltage at the generator's terminals is 240V, then the stepper motor will change the position of the directional rotor blades to the neutral position (Fig. 14a), thus changing the angle of the setting of the main rotor axis to an unfavourable direction relative to the wind direction (Fig. 14b). The return of the rotor axis to the wind direction will occur when the voltage on the generator's terminals drops to 230V or the speed of the main rotor drops to 210 rpm. The tilting gear is driven from the axis of the directional rotor, at the end of which the bevel gear 10 connected to the self-locking worm gear 12 is located. Coupling it with the main bearing structure of the main engine mast 11 make it possible to deflect the axis of the main rotor by a certain angle relative to the wind direction.

Fig. 14. The operating principle of the correcting system (active position of the label of the self-adjusting mechanism): (a) position of the turbine, where the rotor speed exceeds the speed limit and the self-adjusting system is changed to the position of the lodes and starts to work, (b) position, where the self-adjusting system protects against exceeding the rotor speed limit

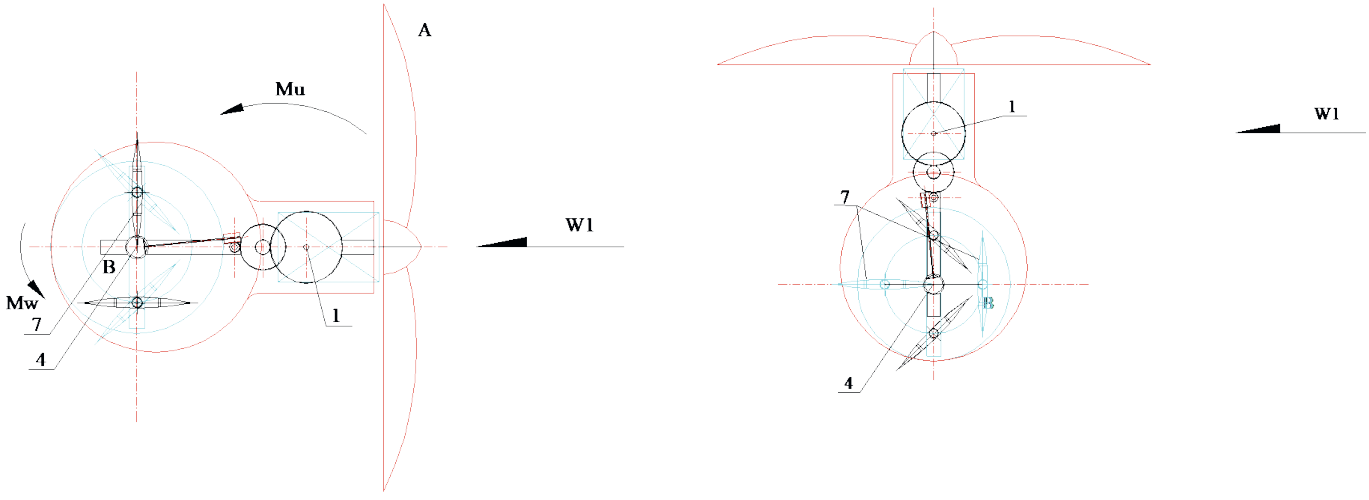

https://doi.org/ 10.37705/TechTrans/e2020009

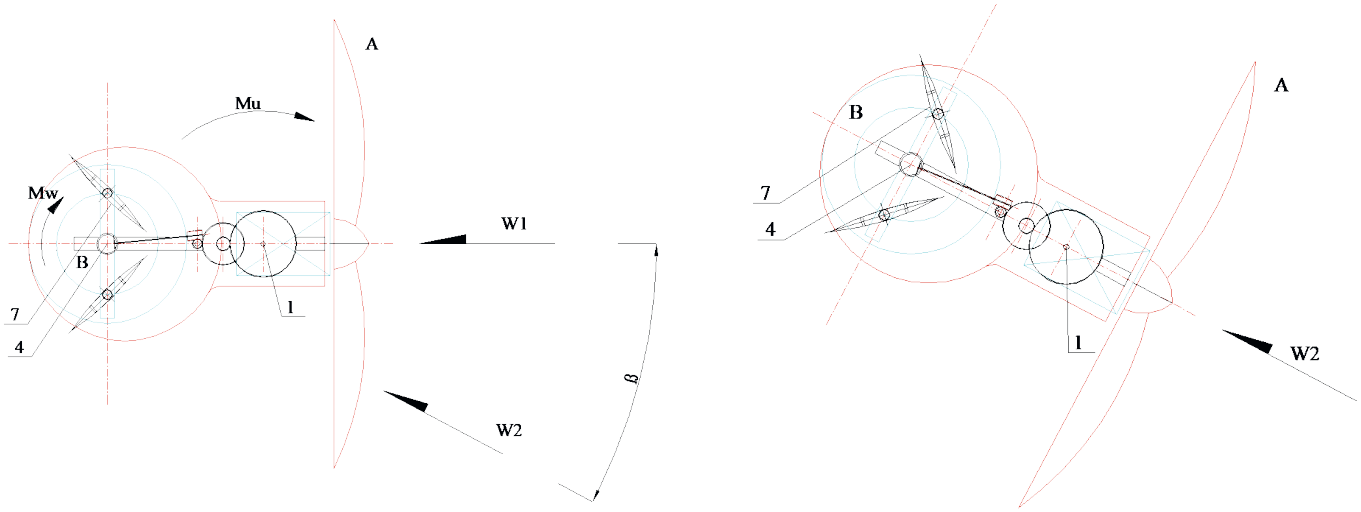

Fig. 15. Method of operation of the self--adjusting system (neutral position of the lobes of the self-adjusting mechanism: (a) change of the wind direction from W1 to W2, (b) new position for the new direction of the wind W2; M_w – torque on the rotor of the self-adjusting mechanism, M_u – torque on the nacelle of the turbine; $M_u = k \cdot M_w$, k – constant

Setting the main rotor to the wind direction is also carried out by the directional rotor B. In Fig. 15a the design solution of the self-adjusting system in the directional equilibrium conditions were shown, for the wind direction marked with the W_1 vector.

When the wind direction W1 is changed, by the angle β to the direction W2, the blades 7 of the self-adjusting mechanism of the directional rotor B performing the planetary motion will cause the rotation of the rotor around the axis 4. The change of the wind direction to W_2 causes the appearance of a rotation torque M_w on the axis of the rotor 4. The resulting torque is transferred to the other components of the self-adjusting system and thus to gear 11 whose axis is coaxial to the axis of the nacelle shaft 1 (torque M_u in Fig. 15a). This causes a deviation in the axis of the jib 3 to the wind direction W_2. The self-adjusting mechanism revolves around the periphery of the fixed wheel 11 and causes the correcting deviation of the main rotor axis by the angle $_\beta$ according to the change of wind direction from W_1 to W_2 as shown in Fig. 15b.

6. Conclusions

A computational procedure for the expected values of the propeller torque and the power per unit area of the turbine blades of a self-adjusting system with two flat blades has been presented. The results allowed an analysis of the rotor, used as the adjusting turbine of the main rotor of a horizontal axis wind turbine (HAWT). The self-adjusting vertical-axis turbine described in the paper provides a continuous setting of the main rotor turbine HAWT (Fig. 13) to the wind direction while simultaneously securing it against strong wind, which could damage the turbine. This solution can work without breaking the generator rotor, as generally used in conventional constructions.

The self-adjusting system works without external or internal electric power and can also protect the turbine against exceeding the permissible speed of the rotor. An equally important feature of this design solution is the virtually maintenance-free operation of the unit with a self-regulating mechanism, which adjusts the turbine gondola position to the direction of the wind.

Specific and important advantages of the new type of self-adjusting unit are summarised in the final remarks as follows: good static and dynamic balancing, the nice geometrical shape of the rotor which can be made of typical materials using standard technology, low mass and cost per unit, easy mounting.

The proposed system can replace solutions, such as a directional rudder or an auxiliary wind motor, which generally requires a generator rotor brake. Changing

the setting of the main rotor of the turbine on the wind direction is conducted in the manner discussed above and has no negative impact on the turbine, while providing good accuracy by directing the main propeller.

References

Hau, E. (2013). *Wind turbines: Fundamentals, Technologies, Application, Economics*. Berlin: Springer Verlag.

Müller, G. F., Jentsch, M., Stoddart, E. (2009). Vertical axis resistance type wind turbines for use in buildings. *Renewable Energy*, *34*, 1407–1412.

Bausas, M. D., Danao, L. A. M. (2015). The aerodynamics of a camber-bladed vertical axis wind turbine in unsteady wind. *Energy*, *93*, 1155–1164.

Ferreira, C. J. S., Van Bussel, G. J. W., Van Kuik, G. A. M., Scarano, F. (2011). On the Use of Velocity Data for Load Estimation of a VAWT in Dynamic Stall. *J. Sol. Energy Eng*, *133*(1), 011006 1–8.

Howell, R., Qin, N., Edwards, J., Durrani, N. (2010). Wind tunnel and numerical study of a small vertical axis wind turbine. *Renewable Energy*, *35*, 412–422.

Ismail, M. F., Vijayaraghavan, K. (2015). The effects of aerofoil profile modification on a vertical axis wind turbine performance. *Energy*, *80*, 20–31.

Li, Q. et al. (2015). Effect of number of blades on aerodynamic forces on a straight-bladed Vertical Axis Wind Turbine. *Energy*, *90*, 784–795.

Edwards, J. M., Danao, L. A. M., Howell, R. J. (2012). Novel Experimental Power Curve Determination and Computational Methods for the Performance Analysis of Vertical Axis Wind Turbines. *J. Sol. Energy Eng*, *134*(3), 031008 63–78.

Hure, N. et al. (2015). Optimal wind turbine yaw control supported with very short-term wind predictions. In *IEEE International Conference on Industrial Technology* (pp. 385–391), Seville.

Xisto, C. M., Pascoa, J. C., Trancossi, M. (2015). Geometrical Parameters Influencing the Aerodynamic Efficiency of a Small-Scale Self-Pitch High Solidity VAWT. *Journal of Solar Energy Engineering*, *138*(3), 10.

Ahmed, S. (2011). *Wind energy: theory and practice*. New Delhi: PHI LearningPvt.

Burton, T., Jenkins, N., Sharpe, D., Bossanyi, E. (2001). *Wind Energy Handbook*. New York: John Wiley & Sons.

Dakin, E., Priyavadan, M., Hopkins, A. (2011). Catching the Wind – An Update on Improved Yaw Alignment. In *Proceedings of EWEA*. Brussels.

Islam, M., Ting, D. S. K., Fartaj, A. (2008). Aerodynamic models for Darrieus-type straight-bladed vertical axis wind turbines. *Renewable and Sustainable Energy Reviews*, *12*, 1087–1109.

Dongran Song, et al. (2017). A novel wind speed estimator-integrated pitch control method for wind turbines with global-power regulation, *Energy*, *138*, 816–830.

Kjellin, J., Eriksson, S., Bernhoff, H. (2013). Electric Control Substituting Pitch Control for Large Wind Turbines. *J. Wind Energy*, 1–4.

Rossander, M., Goude, A., Eriksson, S. (2017). Critical speed control for a fixed blade variable speed wind turbine. *MDPI Energies*, *10*(11), 1–21.

Yang, J. et al. (2016). Comparative studies on control systems for a two-blade variable-speed wind turbine with a speed exclusion zone. *Energy*, *109*, 294–309.

Wei, X., Pan, Z., Liping L. (2015). Wind tunnel experiments for innovative pitch regulated blade of horizontal axis wind turbine. *Energy*, *91*, 1070–1080.

Eriksson, S., Bernhoff, H., Leijon, M. (2008). Evaluation of different turbine concepts for wind power. *Renewable and Sustainable Energy Review*, *12*, 1419–1434.

Pope, K., Dincer, I., Naterer, G. F. (2010). Energy and exergy efficiency comparison of horizontal and vertical axis wind turbines. *Renewable Energy*, *35*, 2102–2113.

https://doi.org/ 10.37705/TechTrans/e2020009

Ryś, J., Augustyn, M. (2015). Patent. *Zespół samonaprowadzania turbiny wiatrowej o poziomej osi obrotu na kierunek wiatru*. P.219834.

Flaga, A., Kłaput, R., Augustyn, M. (2016). Wind tunnel tests of two free-standing lighting protection masts in different arrangements with surroundings roof objects and roof conditions. *Engineering Structures*, *124*, 539–548.

Ryś, J., Augustyn, M. (2013). Innovative construction of 3-component aerodynamic balance. In A. Muc, M. Barski, P. Kedzioria (Eds.), *Advanced Materials in Machine Design – Key Engineering Materials* (pp. 171–177), Trans Tech Pubn 542.

I would like to express my sincere thanks to Prof. Jan Ryś for the valuable tips and suggestions, that contributed to increasing the value of this article.

Wirnik o osi pionowej jako układ regulacji turbiny wiatrowej o poziomej osi

Streszczenie

W artykule zaprezentowano nowatorskie rozwiązanie zespołu samonaprowadzania na kierunek wiatru turbiny wiatrowej o poziomej osi obrotu, składające się z dwułopatowego, karuzelowego wirnika o pionowej osi obrotu i dwupozycyjnego mechanizmu nastawczego. Na podstawie przeprowadzonych badań w tunelu aerodynamicznym wyznaczono wartości współczynników aerodynamicznych łopaty płaskiej wirnika dwułopatowego turbiny naprowadzającej, a ich wartości zobrazowano na wykresach. Przedstawiono procedurę obliczeniową mocy oraz momentu napędowego wirnika zespołu samonaprowadzania w zależności od kąta działania wiatru. Wyniki obliczeń pokazano na wykresach. Zaprezentowano budowę i zasadę działania turbiny naprowadzającej, a także propozycję wykorzystania jej jako zespołu samonaprowadzania na kierunek wiatru z jednoczesnym zabezpieczeniem wirnika głównego HAWT przed nadmiernymi obrotami przy silnym wietrze.

Słowa kluczowe: układ naprowadzenia, turbina wiatrowa o poziomej osi, moment napędowy, turbina wiatrowa o pionowej osi, wirnik wiatrowy

https://doi.org/ 10.37705/TechTrans/e2020009